Prepared for
National Aeronautics and Space Administration
Ames Research Center
Moffett Field, California
Under NASA Grant NSG 2025

UCLA-ENG-7687
SEPTEMBER 1976

OXIDATION OF METALS AND ALLOYS IN CONTROLLED ATMOSPHERES USING IN-SITU TRANSMISSION ELECTRON MICROSCOPY AND AUGER SPECTROGRAPHY

D.B. RAO
K. HEINEMANN
D.L. DOUGLASS

UCLA • SCHOOL OF ENGINEERING AND APPLIED SCIENCE

Oxidation of Metals, Vol. 9, No. 4, 1975

Oxide Nucleation on Thin Films of Copper During *in Situ* Oxidation in an Electron Microscope*

Klaus Heinemann,† D. Bhogeswara Rao,† and D. L. Douglass‡

Received January 2, 1975

Single-crystalline thin films of copper were oxidized at an isothermal temperature of 425°C and at an oxygen partial pressure of 5×10^{-3} Torr in situ *in a high-resolution electron microscope. The specimens were prepared by epitaxial vapor deposition onto polished {100} and {110} faces of rocksalt and mounted in a hot stage inside an ultra-high-vacuum specimen chamber of the microscope. Large amounts of sulfur, carbon, and oxygen were detected by Auger electron spectroscopy on the surface of the as-received films and were removed* in situ *by ion-sputter etching immediately prior to the oxidation. The nucleation and growth characteristics of Cu_2O on Cu were studied. The predominantly observed crystallographic orientations of Cu_2O on {100} and {110} copper films were epitaxial, parallel {100} and {110} orientations, respectively. In addition, a Cu_2O {111} orientation with $Cu_2O\langle 110\rangle // Cu\langle 110\rangle$ was found frequently on {100}-oriented copper films. The distinct particle shapes observed most frequently were square and hexagonal, representing {100} and {111} orientations, respectively. An induction period of about 30 min was found, which did not depend on the film thickness but did depend strongly on the oxygen partial pressure and the oxygen exposure prior to the oxidation. Neither stacking faults nor dislocations were found to be associated with the Cu_2O nucleation sites. The growth of Cu_2O nuclei was found to be linear with time. The experimental findings, including results from oxygen dissolution experiments and from repetitive oxidation–reduction–oxidation sequences, fit well into the framework of an oxidation process involving (a) the formation of a surface-charge layer, (b) oxygen saturation in the metal and formation of a*

*This work was performed at the Ames Research Center and funded by NASA Grants NCA2-OP390-403 and NSG-2025.

†Ames Research Center, NASA, Moffett Field, California.
‡University of California, Los Angeles, California.

supersaturated zone near the surface, and (c) nucleation, followed by surface diffusion of oxygen and bulk diffusion of copper for lateral and vertical oxide growth, respectively.

KEY WORDS: nucleation; epitaxy; nuclei coalescence; growth rates; surface diffusion.

INTRODUCTION

An apparently simple, thermodynamically favorable reaction between a metal and oxygen is often controlled by a complex reaction mechanism. Several stages are involved before the formation of a compact scale of metal oxide on the metal takes place, and the mechanisms that govern the various stages are different. A variety of factors (e.g., temperature, oxygen pressure and residual gas environment, surface preparation, surface impurities, crystallographic surface orientation, crystal defects, and grain boundaries) markedly influence the reaction. The sequence of events that takes place in the interaction of oxygen with a metal has been summarized recently by Ritchie[1] and is schematically represented in Fig. 1.

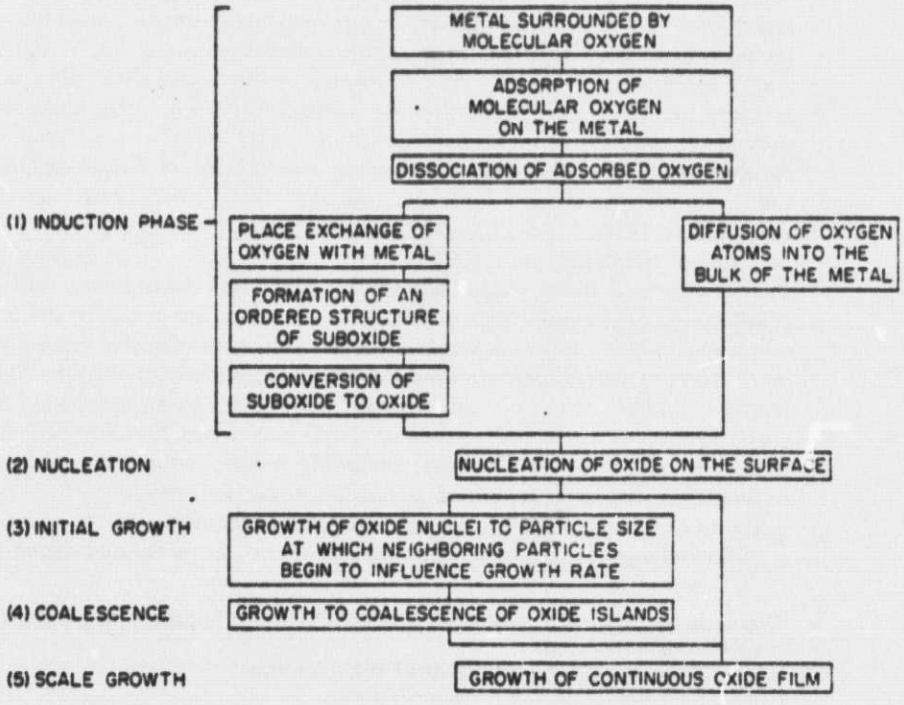

Fig. 1

Very little information is available on the reaction path of the early stages of oxidation, whereas a good deal of understanding has been reached in the growth of scaling layers. The study of the early stages of the oxidation of metals has experienced a renaissance with the advent of new surface analytical techniques. Auger electron spectroscopy (AES), low-energy electron diffraction (LEED), secondary ion mass spectrometry (SIMS), and ion-scattering spectroscopy (ISS) are capable of determining the surface composition with a sensitivity high enough to detect small fractions of atomic layers on the surface. These techniques, however, display very poor lateral resolution which is necessary for the detection of the size and distribution of surface heterogeneities and the orientation of oxidation products. Most valuable information of this sort can be obtained with a high-resolution transmission electron microscope. The present studies were undertaken to gain more insight on the reaction path and mechanism between chemisorption and oxide scale formation. Some results of our *in situ* work on the low-pressure oxidation of clean, single-crystalline copper films are reported in this paper. A high-resolution transmission electron microscope equipped with an ultra-high-vacuum (UHV) specimen chamber, a hot stage, and argon-ion specimen cleaning facilities was employed in this investigation. Copper was chosen for the general simplicity of its metal–oxide system, the relative ease of copper specimen preparation, the considerable amount of data for the later stages of oxidation, and easily detectable oxidation products for our experimental conditions.

Menzel and Stossel[2] first reported that isolated copper oxide nuclei are formed on copper when the oxidation is carried out at low oxygen partial pressures. Grønlund and Bénard[3] later classified the initial oxidation process in three distinctive stages: (i) the induction period during which no oxide appears as nuclei; (ii) a sudden nucleation period during which distinct oxide nuclei appear; and (iii) the growth period during which the volume of the nuclei increases by a lateral growth mechanism. The investigation was carried out employing an optical microscope and the details were limited due to poor lateral resolution. Subsequently, several other investigators studied the early oxidation behavior of single-crystalline as well as polycrystalline copper using electron and optical microscope techniques.[4–11] However, the results of those investigations are not always consistent due to insufficient control over some of the vital experimental parameters such as surface cleanliness, residual gas environment, and gaseous pretreatment of the specimen. It is known, for example, that surface contamination effects an increase in nuclei number density.[12] It is also known that during heat treatment carbon and sulfur, which are usually present as impurities in the metal, migrate to the surface, and it is conceivable that they might significantly alter the oxidation behavior. The most effective way of removing such surface impurities is by ion sputtering.[13,14]

Investigators who studied the oxidation of thin films customarily annealed the specimen in hydrogen, in order to remove the adsorbed contaminants which would have accumulated during the process of preparation and handling the films. Swanson and Uhlig[15] examined the influence of such a gaseous pretreatment and reported that submicroscopic faceting resulted due to surface treatment with hydrogen and nitrogen, leading to changes in orientation relationships and oxidation rates. This might, conceivably, be one of the causes for the lack of consistency in the orientation relationships of the oxide particles on {100} copper films.[16] We have, therefore, decided to study the initial oxidation behavior of sputter-cleaned, single-crystalline copper films without pretreating them with hydrogen. The surfaces were exposed to hydrogen only in those cases where the effect of hydrogen pretreatment on the oxidation was investigated.

EXPERIMENTAL

{100}-oriented, single-crystalline copper films with an average thickness of 800 Å were prepared by epitaxial vapor deposition of copper from an electron beam evaporation source onto the {100} face of sodium chloride. NaCl crystals obtained from the Harshaw Co. were used as substrates. Substrate surfaces having 13-mm edge lengths were obtained by sectioning the crystal at an appropriate angle using a diamond-impregnated, stainless steel wire cutter. The sawed surface was then carefully metallographically polished, using successively the finest abrasive papers. It was then further polished on a glass slab with alumina powder suspended in ethanol and finally with a paste of magnesium carbonate powder suspended in ethylene glycol. The surface was then washed quickly with ethanol and dried quickly with hot air. An analogous procedure was adopted by Wakashima, Fukamachi, and Nagakura,[17] who succeeded in preparing a step-free, single-crystalline copper film. {110}-oriented, single-crystalline copper films were prepared in a similar manner by epitaxial deposition on {110} NaCl faces. The substrate was then suspended in the center of a resistance-heated furnace in a bell jar deposition system which was subsequently evacuated to a vacuum better than 10^{-7} Torr. The substrate temperature was maintained at 300°C. Copper was evaporated at an automatically controlled deposition rate of 10 Å sec^{-1} with a SLOAN (OMNI 11) rate monitor in conjunction with an oscillating quartz crystal microbalance. The film was cut into 2 × 2 mm^2 pieces and collected on 200-mesh copper grids.

The surface of the resulting films was found relatively smooth, and replicas made by shadow casting with a platinum–carbon alloy did not show any significant surface roughness. The films were then oxidized in the controlled vacuum specimen chamber of a high-resolution transmission

electron microscope. The entire system, which was basically described in an earlier paper by Moorhead and Poppa,[18] was rebuilt using a Siemens Elmiskop 101 which helped to yield micrographs with better resolution and contrast. The new microscope system is shown in Fig. 2.

The copper film was then mounted in the specimen stage which could be heated to a desired temperature. The specimen chamber section of the microscope was mildly baked to degas the adsorbed gases and pumped down to a vacuum in the 10^{-9} Torr range. The specimen stage was then heated to a temperature of 425°C and annealed (3–4 hr) until the film surface was smooth. The upper surface of the film was then cleaned by argon ion-sputter etching. The etching was carried out for about 10 min during which a mass corresponding to a thickness of 200 Å might have been removed. During the treatment of the surface with gases, the orb ion pumps (OIP) were not operated. The system was, instead, differentially pumped with a well-trapped oil diffusion pump and a titanium sublimation pump.

After sputter cleaning the surface, oxygen was admitted and the system was equilibrated to a pressure of 5×10^{-3} Torr and was maintained constant by pumping against an adjustable leak. Pressure equilibrium was attained within 2–3 min. The oxygen partial pressure as well as the temperature

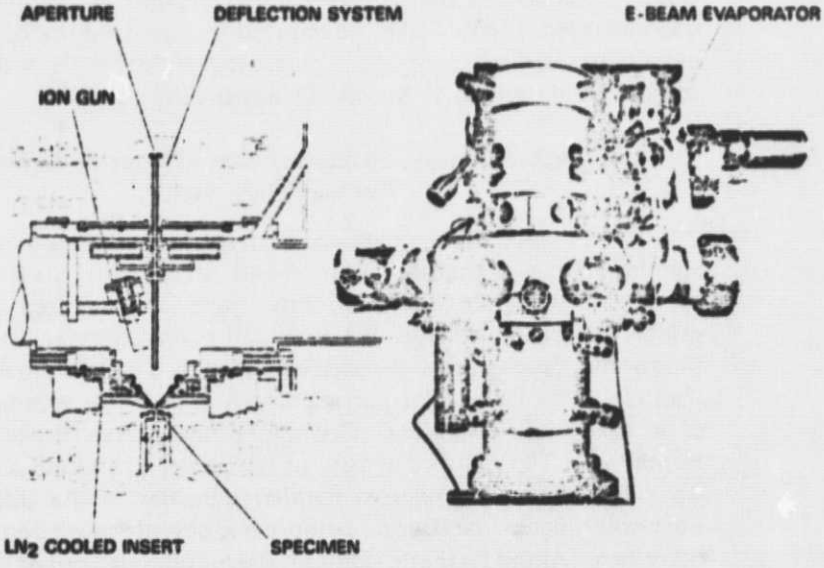

Fig. 2. Cross section (left) and front view (right) of the center portion of the ultra-high-vacuum specimen chamber and the electron microscope.

(425°C) were maintained constant during the oxidation, and transmission electron micrographs, selected area diffraction patterns, and selected zone dark field (SZDF) micrographs[19] were taken constantly at desired intervals. In order to avoid a possible damage of the film by excessive electron irradiation, the reference area used to compute the oxidation results was viewed only to take the photographs. The general viewing was performed at a different specimen area, preferably using an image intensifier system[20] which significantly reduced the necessary probe current. The results were highly reproducible, provided the critical experimental conditions including surface pretreatment of the samples were kept constant.

RESULTS

Induction Period

The typical growth of Cu_2O on {100}-oriented copper under the conditions described earlier is represented in the micrographs of Fig. 3. No evidence of oxide particles was visible either in the selected area diffraction (SAD) patterns or in the transmission electron micrographs until an oxidation period of approximately 30 min had elapsed. The oxide particles nucleated suddenly and are indicated by arrows in Fig. 3(b). The induction period could be reduced if the oxygen partial pressure in the reaction chamber was increased. It could also be reduced by exposing the copper film to an oxygen atmosphere prior to the beginning of the regular oxidation (see the section, Oxidation of As-Received Copper Films, p. 389).

Number Density, Shape, and Crystallographic Orientation of the Oxide Nuclei

Two distinct, different shapes of oxide nuclei, namely, square particles and hexagonal crystallites, were found to nucleate on a {100}-oriented copper substrate. In addition, some particles nucleated which did not exhibit a particular shape. We shall call them "circular" particles. At the time of their appearance, the area occupied by a square particle was greater than the area of a circular particle which in turn was greater than the area of a hexagonal crystallite. The approximate area ratios were 10:6:1, respectively. The number density of the nuclei was found to be $2 \times 10^8 \pm 0.5 \times 10^8\ cm^{-2}$. The relative number densities of the different particles were nearly equal, the squares being found slightly more frequently than the other two. During further oxidation, the number density of nuclei remained constant (see Fig. 3).

The predominantly observed epitaxial relations for the square particles were Cu_2O {100}//Cu {100} and Cu_2O {110}//Cu {110}. An epitaxial orienta-

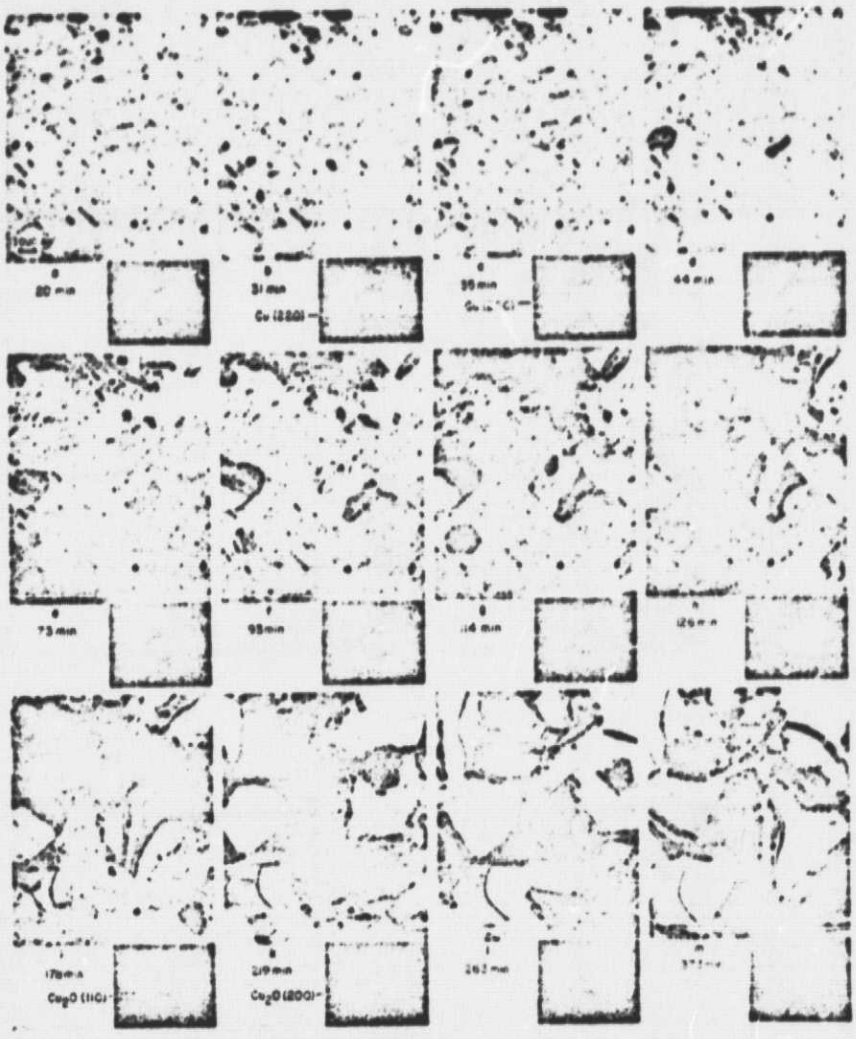

Fig. 3. Oxidation series of a thin, sputter-cleaned, {100}-oriented Cu film at 425°C and $P_{O_2} = 5 \times 10^{-3}$ Torr.

tion of Cu_2O {111}//Cu {100} with Cu_2O ⟨110⟩//Cu ⟨110⟩ was observed for the hexagonal particles. The high degree of epitaxy is demonstrated in Fig. 4(d) where three micrograph exposures with different defocus settings are superimposed in the {110} SZDF mode.[19] The direction of the resulting shift of the reflection images is normal to {110} lattice planes of the diffracting crystallites. The predominant existence of 90° and 60° symmetries marks the degree of {100} and {111} epitaxy.

Fig. 4. Thin, {100}-oriented copper film: (a) immediately after sputter cleaning and thinning, and (b)–(d) after 74 min oxidation at 425°C and $P_{O_2} = 5 \times 10^{-3}$ Torr. The micrographs (c) and (d) are Cu_2O {110} selected zone dark field (SZDF) micrographs; (d) is a superposition of three SZDF micrographs at different defocus settings.

As can be noted from micrographs 3(d) and 3(f), a square particle extending to and beyond a small hole in the copper film retained its normal growth pattern, virtually unaffected in growth direction and speed by the hole. The growth of {111}-oriented nuclei was considerably different than that of {100}-oriented crystallites, as noted in micrographs 3(e) to 3(h). First, the outer appearance, i.e., the interface between the oxide and the copper film, of these nuclei differed from that of {100} crystallites. Second, particle outlines similar to stacking-fault fringes were not observed for {111} nuclei, whereas they had been noted in high-magnification micrographs of {100} nuclei. Third, SZDF micrographs of these early-stage {111} crystallites did not reveal any oxide reflections, as can be seen in Fig. 5 which depicts the oxidation stage of Fig. 3(d). The SZDF exposure [Fig. 5(b)] was taken with the Cu_2O {110} zone into which normally both {100}- and {111}-oriented bcc crystals are expected to reflect. In later SZDF examinations, the reflections of this {111}-oriented Cu_2O particle were found to be present.

The last four micrographs (i)–(m) of Fig. 3 represent the stage of oxidation between approximately 3 and 6 hr. At the end of this period over 70% of the film area is covered with oxide. The diffraction patterns now clearly indicate the predominance of the {100} orientation with a high degree of epitaxy.

Nucleation Sites

The particle on the left side of Fig. 3(b)—indicated by an arrow—nucleated on a dislocation loop site, whereas the square particle seems to be surrounded by stacking faults. However, no stacking fault had been

Fig. 5. Enlargement of Fig. 3(d) and corresponding {110} SZDF micrographs.

observed before the oxidation at the particular particle site, and the stacking-fault-like contours move with increasing particle size [*cf.* micrographs 3(c), 3(d), 3(e)]. It can, therefore, be concluded that the stacking-fault-like fringes mark the oxide–metal interface, and it can be inferred that these interfaces are parallel to metal and oxide {111} planes. A thorough examination of all our results, so far, indicates that neither stacking faults nor dislocations are associated with the nucleation sites.

Growth Characteristics

Oxide particle growth occurred laterally as indicated in micrographs 3(c) and 3(d), which were taken after an oxidation period of 35 and 44 min, respectively. Already at a very early stage of oxidation [comparable to the stage depicted in Fig. 3(b), shortly after the end of the induction period] the oxide particle thickness is comparable to the total film thickness. This can be confirmed with SZDF studies.[19] The Cu_2O {220} SZDF image [Fig. 6(b)] clearly shows the Cu_2O crystallites, whereas the Cu {220} SZDF image [Fig. 6(c)] leaves dark blanks covering the entire area of the Cu_2O crystallites, which is an unambiguous proof of the absence of free copper within these areas. A similar conclusion was reached earlier by Brockway and Rowe[7] by treating the oxidized film with a dilute acid.

Annealing of Oxidized Films

When, after an extensive oxidation treatment, the oxygen partial pressure in the reaction chamber was reduced to the 10^{-10} Torr level while the specimen temperature was kept unchanged, significant changes became

Fig. 6. Thin, oxidized {100} copper film: (a) in bright field, (b) Cu_2O {220} dark field, and (c) Cu {220} dark field.

apparent in the image after several hours. A large number of small, irregularly shaped features had formed on the Cu_2O crystallites, with the density increasing sharply near the oxide–metal interfaces [see Fig. 7(a)]. Upon resumption of oxidation at this stage, it was noticed that first, these features slowly disappeared: second, the oxide crystals began to grow laterally again [Fig. 7(b)]; and third, after an exposure of 150 min [see Fig. 7(b)], which corresponds in terms of oxygen exposure to stage (i) in Fig. 3, a very large number of small polycrystalline Cu_2O particles developed, obviously both on the Cu_2O crystallites and on the unoxidized copper areas. The number density of this polycrystalline deposit was 2×10^{11} cm^{-2}, which is three orders of magnitude greater than the number density of the primary epitaxial Cu_2O crystals. Figure 7(c) depicts a much further progressed oxidation stage, where these polycrystalline oxide particles have grown to an area coverage close to unity. At this time, the copper film had been almost completely oxidized, as noted from the missing Cu reflections in the SAD pattern.

Oxidation of As-Received Copper Films

A similar oxide nucleation behavior was found when copper films were oxidized without prior argon-ion sputter-cleaning treatment. Figures 8(a) and 8(b) show a typical area of an as-received, annealed but not sputter-cleaned {100} Cu film prior to and after 60 min oxygen exposure at our standard conditions of 425°C and 5×10^{-3} Torr oxygen partial pressure. The oxide formation with very high particle number density is clearly visible in Fig. 8(b), and so is the fine polycrystalline character of the oxidation product in the SAD pattern. The film was further oxidized for 90 min more (for a total of 150 min oxidation), and lateral growth of these initially extremely small oxide nuclei as well as an increase of intensity of the Cu_2O rings in the SAD pattern were observed. The film was then, immediately following the end of the oxygen exposure, subjected to a short (4 min) argon-ion etching treatment, and another oxidation at the previous experimental conditions was initiated. During the etching process, all evidence of the oxide disappeared very rapidly in the transmission electron image and in the diffraction pattern, and the nucleation of regular, epitaxial {100}-oriented oxide crystallites was noticed immediately after admitting the oxygen, with a negligible induction period [see Fig. 8(c), taken after 36 min of renewed oxygen exposure].

Oxidation–Reduction–Oxidation Sequences

Successive oxidation–reduction–oxidation experiments were carried out and observed at the same specimen area to gain information about the mechanism of hydrogen reduction of a partially oxidized single-crystalline

Fig. 7. Strongly oxidized copper film: (a) after several hours of annealing at 425°C and $P_{O_2} < 10^{-10}$ Torr, (b) after 150 min renewed oxidation at $P_{O_2} = 5 \times 10^{-3}$ Torr, (c) after 330 min oxidation.

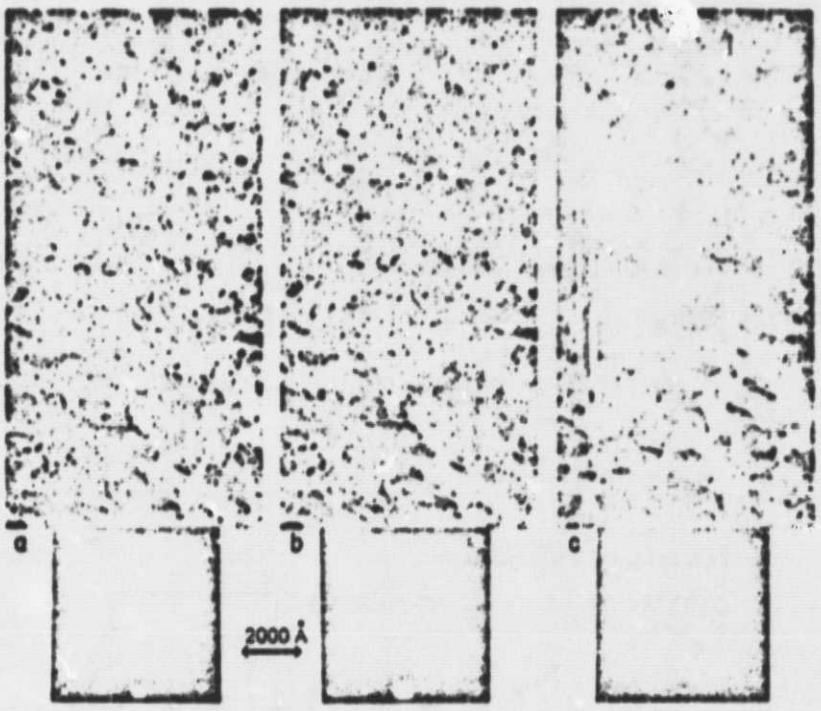

Fig. 8. Thin, {100}-oriented copper film: (a) as-received. (b) after 60 min oxidation at 425°C and $P_{O_2} = 5 \times 10^{-3}$ Torr. (c) after 150 min oxidation, 4 min sputter etching, and 36 min renewed oxidation.

copper film and about the character of oxide nucleation sites. Figure 9 gives the experimental observations. The micrograph in Fig. 9(a) shows a sputter-cleaned surface area before oxidation: Figs. 9(b), 9(c), and 9(d) show the same area after consecutive steps of oxidation under the standard conditions for 20, 47, and 61 min of oxygen exposure, respectively. The sample was then exposed to a hydrogen environment of 8×10^{-4} Torr partial pressure. An exposure of only 7 min reduced the size of the oxide crystallites by a factor of about 2 in volume, as can be seen in Fig. 9(e) and the schematic summary 9(f). The reduction was completed after 10 min more of hydrogen exposure. General observations during the reduction process include a well-defined but usually less straight or less crystallographically oriented interface between oxide and metal, an obviously considerably thinner metal film as a reduction product in the reduced areas when compared to the appearance of the film prior to oxidation, a perfectly smooth transition from the unoxidized to the reduced film areas without evidence of grain or low-angle boundaries, and a tendency of the new, thin copper film areas to

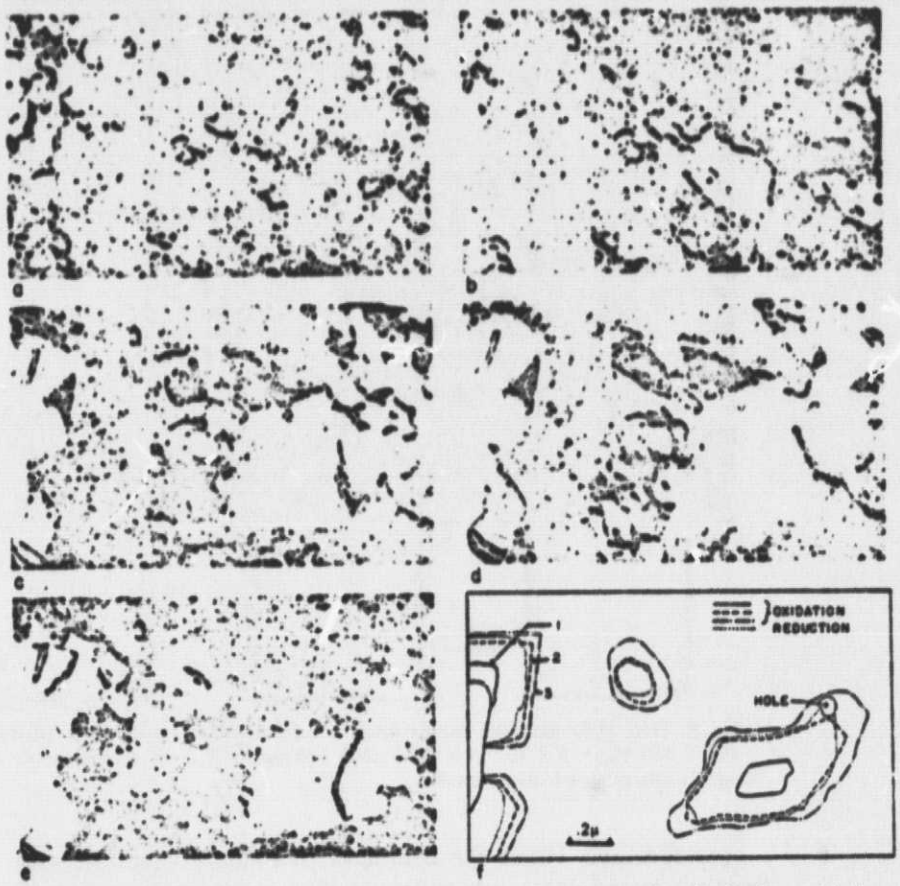

Fig. 9. Thin, {100}-oriented copper film: (a) before oxidation. (b)–(d) during oxidation. (e) during hydrogen reduction. (f) is a schematic summary of the particle outlines in (b)–(e).

break up, which is believed to be due to surface tension effects. Renewed oxidation immediately following the reduction process resulted in the nucleation of the usual epitaxial oxide crystallites at random, different locations, similar to the first oxidation but with a considerably shorter induction period.

DISCUSSION

Induction Period

The induction period is probably the least understood stage in the entire oxidation process. It is conceivable that for a clean copper surface the first step in the induction phase is a chemisorption of a layer of oxygen

on the surface. Since a clean metallic surface is very reactive, this initial coverage can be expected to occur rapidly, with a sticking coefficient close to unity. LEED measurements[24] have, for example, revealed that the first significant oxygen adsorption evidence on a {110} copper surface occurs after only 3×10^{-8} Torr min oxygen exposure. It is, therefore, safe to assume that at an oxygen partial pressure of 5×10^{-3} Torr, that prevailing in our experiments, the initial oxygen surface coverage occurs instantaneously. The fact that an induction period of approximately 30 min was reproducibly observed must, therefore, indicate that the oxide nucleation process is not surface-controlled. It must, instead, be controlled by conditions in the bulk of the copper specimen, preferably close to the surface, and it is reasonable to think that oxygen diffusion into the copper and the establishment of an oxygen-saturated zone near the surface are necessary requirements. This oxygen-saturated zone may, however, be relatively narrow when compared to the entire film thickness, which would explain why other authors[5,7,23] found almost the same induction period in their experiments, although their specimen thickness was considerably greater.

The above assumption that a critical oxygen concentration has to be established below the surface before the conditions for oxide precipitation are fulfilled is further supported by the results of our oxidation experiments with as-received copper films (see p. 389), as well as by our successive oxidation–reduction–oxidation experiments (see p. 389). In both cases, a copper film was exposed to an oxygen environment until clear evidence of oxide was noted in the SAD pattern and the electron image. The oxidation process was then interrupted and the oxide was removed by sputter etching or by reduction in hydrogen until all evidence of oxide had disappeared. However, this short ion-etching or hydrogen treatment was found not to significantly affect the oxygen concentration inside the copper film, which remained, therefore, close to the solubility concentration. Renewed exposure to oxygen resulted in both cases in immediate oxide formation at randomly different sites and without any noticeable induction period.

Number Density, Shape, and Crystallographic Orientation of the Oxide Particles

The number density of oxide crystallites epitaxially grown on {100} copper faces (2×10^{8} cm^{-2}) is in fair agreement with earlier reported data.[5,7] Considerable disagreement exists, however, in the shape and crystallographic orientation of the observed oxide nuclei. Whereas in earlier work[5,7,23] a triangular, pyramidal shape and a {111} orientation of the oxide particles were reported as the main results for oxidation on {100} copper, we find a predominant parallel {100} orientation, associated with square particle

shapes. Even in those cases when oxide crystallites have a {111} orientation, we find hexagonal rather than triangular outlines and a uniform particle thickness rather than pyramidal shapes. A comparison of the experimental conditions to clarify some of the discrepancies indicates major differences in sample thickness and gaseous pretreatment. Most investigators used bulk copper (for example, Refs. 5 and 21) and subjected their samples to a thorough hydrogen annealing treatment prior to the oxidation. Such gaseous pretreatment can lead to submicroscopic faceting and consequently to significant changes in orientation relationships and oxidation rates,[15] as was already pointed out earlier in this report.

We have tried to approach the conditions of such investigations by using a thicker copper film and annealing it in hydrogen prior to the oxidation. Under these conditions, we were able to reproduce the pyramidal shape of the nuclei (Fig. 10). Our *in situ* growth observations and SZDF studies have, however, cast much doubt on the identification of these nuclei as {111}-oriented oxide crystallites. Work is going on to clarify their exact nature, a task which will probably not be completed before a sensitive surface analysis tool with a spatial resolution high enough to depict these small crystallites

Fig. 10. {100}-oriented, 1200-Å-thick copper films, annealed in hydrogen and oxidized for 62 min at 425°C and $P_{O_2} = 5 \times 10^{-3}$ Torr.

can be employed. Such a system, an Auger microprobe with depth profiling capabilities, is currently under construction in our laboratory.

Oxide Nucleation Sites

Typical number densities of stacking faults in our {100} copper films were 5×10^9 cm^{-2}. Although this number is considerably higher than the regular oxide nuclei number density, we did not observe any oxide nucleation at stacking fault sites beyond what can be considered as random coincidence. The same holds true for dislocations. It can be concluded, therefore, that for sputter-cleaned {100} surfaces of copper, the surface energy inhomogeneities at stacking faults and surface-intersecting dislocations are not high enough to act as preferred oxide nucleation sites. The nucleation occurs, therefore, at random sites. This conclusion is supported by oxidation–reduction–oxidation sequences (see p. 389) in which the renewed oxide nucleations repeatedly occurred at random, different sites. Similar results were reported earlier for the growth of nickel oxide on nickel.[25] However, our results disagree with an earlier report by Brockway and Rowe[7] that the number of nuclei associated with stacking faults was approximately 4 times the number expected for a random distribution.

The only time when we noticed preferential nucleation was after prolonged ion etching to the extent that through-thickness holes had formed in the copper film. Preferential nucleation was then observed at the edges of the holes in the film (see Fig. 4) in addition to the normal nucleation at random sites. This result can be explained tentatively by a different surface orientation of the substrate film at hole edges, resulting from the etching process.

Growth Characteristics

Growth Rate

The outlines of the crystallites in Fig. 3 are summarized in Fig. 11, demonstrating their growth during successive oxidation time intervals. It is evident that the particle growth occurred predominantly in the direction of unoxidized copper and that the rate is affected by the surrounding particles. Therefore, the tendency for coalescence of these nuclei is low until the entire copper is oxidized.

For a more detailed analysis, the surface areas of the three differently shaped particles (square, hexagonal, circular) are plotted independently as a function of oxidation time and are shown in Fig. 12. The growth of all these particles shows a linear dependence with time except for the hexagonal particles (denoted by triangles in the figure) for which the early growth rates deviate from linearity. This could be due, as mentioned earlier, to the fact

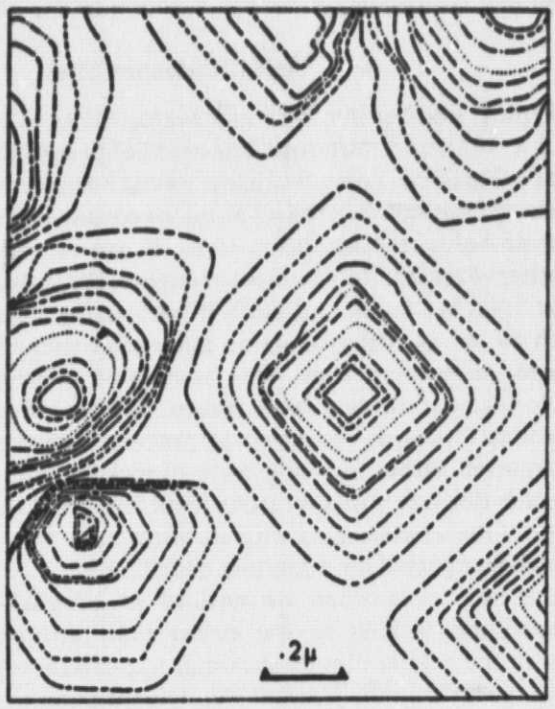

Fig. 11. Schematic summary of oxide crystallite outlines at different stages of oxidation, taken from Fig. 3.

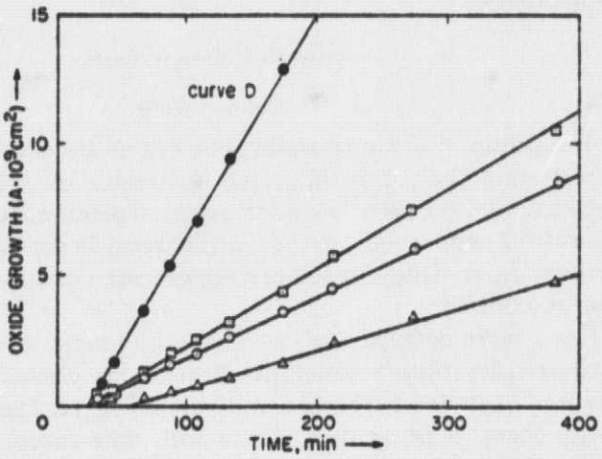

Fig. 12. Area (A) of square, circular, and hexagonal (denoted by triangles) oxide crystallites vs oxidation time. The solid circles (labeled curve D) represent the total area coverage vs time characteristic.

that this particle did not initially extend through the entire depth of the film, and some copper remained beneath the particle. In such a case, part of the atom flux arriving at the particle edge might be consumed in the oxidation of the interior copper present, resulting in a slower lateral growth. The beginning of linearity in the growth rate coincides well, indeed, with the time at which SZDF observation indicated completion of the through-thickness oxidation of this particle. Since the surface area occupied by this particle was initially small, when compared to the rest of the oxide crystallites, the sum of all areas also shows a linear time dependence (curve D). Using the method of least squares, we calculated the slope of the growth curves in Fig. 12. The resulting growth rates are given in Table I. The extrapolation of the calculated linear function for the sum of all areas (curve D) to $A = 0$ gives $t_0 = 27$ min as an induction period, which is in good agreement with the experimental observations. The value obtained for the overall growth rate of the oxide (1.5×10^{-12} cm^2 sec^{-1}) is in fair agreement with the value reported by Bénard *et al.*[11] (2×10^{-11} cm^2 sec^{-1}). The growth rate of the {100}-oriented particle is nearly twice that of the {111}-oriented particle. The same ratio of 2:1 is found in the distances of the {100}- and {111}-oriented particles to their nearest neighbors. One can, for example, measure in Fig. 11 that the distance from the center of the square particle to the center of the nearest neighboring particle is nearly 1 μm, whereas for the hexagonal particle the corresponding distance is only 0.5 μm. This indicates that the growth rate of the oxide nuclei may be independent of the epitaxial relationships and mainly determined by the diffusion of oxygen toward the growing particles which in turn is dependent on the distances to the nearest neighboring particles.

The overall growth rate of the nuclei measured in this study was found to be nearly identical to that determined by Jardinier-Offergeld and Bouillon[23] although the two techniques were quite different. An application of the model proposed by Rhead[22] involving surface diffusion was made in order to calculate a surface diffusivity. The value obtained, 10^{-11} cm^2 sec^{-1}, was about four orders of magnitude less than experimental values measured by Bradshaw *et al.*[26] for copper on copper in 5×10^{-5} Torr of oxygen.

Table I

Particle shape	Growth rate, cm^2 sec^{-1}
Square, {100}	4.9×10^{-13}
Circular	4.0×10^{-13}
Hexagonal, {111}	2.5×10^{-13}
Total	1.5×10^{-12}

No surface diffusivities have been reported either for oxygen on copper or for oxygen on an adsorbed oxygen layer on copper. The inferences to be made from the calculations are that (a) the model does not apply under the boundary conditions chosen and (b) the diffusing species is unknown.

Growth Mechanism

In accordance with the discussion on the induction period (p. 392), it is believed that the nucleation and growth of Cu_2O on thin copper films involves the following mechanism: First, a thin adsorption layer of oxygen atoms adheres rapidly at the surface. An electron exchange takes place, resulting in the formation of some kind of a surface-charge layer. Second, oxygen–metal exchange takes place until an oxygen supersaturation is reached near the surface. Third, oxide nucleates in the supersaturated region of the film. The surface-charge effects become negligible at the sites of the oxide nuclei, surface diffusion of oxygen toward the oxide particle sites begins, and copper diffuses simultaneously through the oxide to the surface. Thus, lateral growth of the oxide nucleus is manifested by surface diffusion, and vertical growth by copper diffusion through the oxide.

The vertical and lateral growth rates can be of different magnitudes, depending on the diffusion rates of copper through Cu_2O and of oxygen near the Cu_2O–Cu interface into the bulk. The difference in vertical growth rate which we observed for the {111}- and {100}-oriented oxide crystallites (see the section, Growth Characteristics, on p. 388) can be explained on the basis of this mechanism by a faster copper ion diffusion through the oxide in the {100} direction when compared to diffusion in the more densely packed {111} direction.

The experimental finding that through-thickness holes in the copper film did not greatly influence the oxide growth behavior can now also be easily understood. Since the attainment of a zone supersaturated with oxygen is required only near the surface, and since the lateral growth mechanism calls for oxygen diffusion rather than copper diffusion to the place of growth, variations in copper film thickness are expected to cause the respective variations in oxide crystal thickness rather than variations in the lateral growth rate. This was observed in our experiments. Holes which were present before oxidation remained holes throughout the entire oxidation process (see Fig. 3), and primary local thickness variations in the copper film were reproduced in the oxide film.

During their growth, the oxide crystallites maintain their original shape and their usually perfect epitaxial alignment. Consequently, the boundaries between coalescing oxide crystallites at a later stage of oxidation are expected to be of a low-angle type.

Annealing of Oxidized Films

The first attempts to explain the nature of the small, irregularly shaped features which were observed on the Cu_2O crystallites after several hours of annealing at low oxygen partial pressure [see the section, Annealing of Oxidized Films, p. 388, and Fig. 7(a)] indicated that they must be interpreted as voids (in thin oxide areas) or locations of considerably thinner oxide (in thicker oxide crystals). Simmons, Mitchell, and Lawless[24] studied the interaction of oxygen with single-crystal surfaces of copper with LEED and HEED and found repeatedly, in agreement with an earlier suggestion by Mitchell and Lawless,[5] that a considerable amount of oxygen went into solution in the bulk copper crystal upon annealing at temperatures up to 800°C. The observed void-like features could be explained on the basis of such an oxygen dissolution process, forming clusters of missing atoms sites in the oxide. The increased number density of the observed voids near the edges of the oxide crystallites could also be accounted for easily. On the basis of this interpretation, an assumption made earlier in this paper (see the section, Induction Period, p. 392) can be strengthened further. At no time during the oxide nucleation and growth process does the concentration of oxygen dissolved in the copper film have to reach the saturation concentration throughout the film, because obviously a considerable additional amount of oxygen could go into solution during the annealing process.

Oxidation of As-Received Copper Films

It is believed that the unusual oxidation behavior on the as-received thin-film copper surface (Fig. 8) is due to contamination of the surface. It is well known that even a thin adsorbed layer of contaminants can change the surface energy conditions so drastically that epitaxial relationships between an overgrowth (e.g., oxide) and the substrate are substantially altered. Diffusion constants on and through such a layer can also be significantly different from the respective values on clean substrates.

We subjected copper films similar to the specimens used in the oxidation experiments to an Auger depth profiling test and found extremely large carbon and sulfur peaks on the as-received film surface, in addition to a large oxygen peak. The relative heights of the copper peaks are comparatively low. The sulfur, oxygen, and carbon peaks decreased rapidly during sputter etching. After an etching time of 5 min, corresponding to an average material removal of about 50 Å, the peak heights of sulfur, oxygen, and carbon were reduced to 2%, 6%, and 10% of their original values, respectively. After 5 min more of etching, all sulfur, oxygen, and carbon peaks had disappeared in the Auger signal. Meanwhile, the signal of copper had increased manyfold.

It is, therefore, clear that an enormous surface contamination is present on the as-received samples and that careful cleaning of the surface is absolutely essential if meaningful and reproducible results are to be obtained.

ACKNOWLEDGMENTS

We are indebted to Dr. Helmut Poppa and Mr. Dell Williams of the Materials Science Branch, Ames Research Center, for stimulating discussions during the course of this work. Thanks are also due to Mr. Dale Moorhead for performing the Auger depth profiling experiments and to Mr. Dan Magan for his skillful technical assistance.

REFERENCES

1. I. M. Ritchie, "The Oxidation of Evaporated Metal Films," in *Chemisorption and Reactions on Metallic Films*, Vol. 2, J. R. Anderson, ed. (Academic Press, London and New York, 1971), p. 260.
2. E. Menzel and W. Stossel, *Naturwissenchaften* **41**, 302 (1952).
3. F. Grønlund and J. Bénard, *C. R. Acad. Sci.* **240**, 624 (1955).
4. E. Menzel and M. Kopp, *Surf. Sci.* **2**, 376 (1964).
5. D. F. Mitchell and K. R. Lawless, Proceedings of the Paint Research Institute, 43rd Annual Meeting of the Federation of Societies for Paint Technology, Atlantic City, N.J. (October 29, 1965).
6. K. R. Lawless and D. F. Mitchell, *Mem. Sci. Rev. Metall.* **62**, 27 (1965).
7. L. O. Brockway and A. P. Rowe, *Fundamentals of Gas–Surface Interactions* (Academic Press, Inc., New York, 1967), pp. 147–160.
8. A. P. Rowe and L. O. Brockway, 27th Annual EMSA Meeting (1969), p. 118.
9. L. O. Brockway, R. B. Marcus, and A. P. Rowe, *Proceedings of the Conference on Single Crystal Films* (Pergamon Press, New York, 1964).
10. T. Homma, T. Yoneoka, and S. Matsunaga, private communication.
11. J. Bénard, F. Grønlund, J. Oudar, and M. Duret, *Z. Elektrochem.* **63**, 799 (1959).
12. E. Menzel and K. Niederauer, *Acta Metall.* **10**, 985 (1958).
13. T. L. Bradley and R. E. Stickney, *Surf. Sci.* **38**, 313 (1973).
14. K. Heinemann and H. Poppa, *J. Vac. Sci. Technol.* **10**, 22 (1973).
15. A. W. Swanson and H. H. Uhlig, *J. Electrochem. Soc.* **118**, 1325 (1971).
16. K. Lawless and A. T. Gwathmey, *Acta Metall.* **4**, 153 (1956).
17. K. Wakashima, M. Fukamachi, and S. Nagakura, *Jpn. J. Appl. Phys.* **8**, 1167 (1969).
18. R. D. Moorhead and H. Poppa, Proc. 27th EMSA Meeting (1969), p. 116.
19. K. Heinemann and H. Poppa, *Appl. Phys. Lett.* **20**, 122 (1972).
20. K. Heinemann and H. Poppa, Proc. 30th EMSA Meeting (1972), pp. 612 and 614.
21. F. Grønlund, *J. Chem. Phys.* **53**, 660 (1956).
22. G. E. Rhead, *Trans. Faraday Soc.* **61**, 797 (1965).
23. N. Jardinier-Offergeld and F. Bouillon, *J. Vac. Sci. Technol.* **9**, 770 (1972).
24. G. W. Simmons, D. F. Mitchell, and K. R. Lawless, *Surf. Sci.* **8**, 130 (1967).
25. K. Heinemann and H. Poppa, Proc. 31st EMSA Meeting (1973), p. 30.
26. F. J. Bradshaw, R. H. Brandon, and C. Wheeler, *Acta Metall.* **12**, 1057 (1964).

IN-SITU ELECTRON MICROSCOPE STUDY OF THE OXIDE/METAL (Cu_2O/Cu) INTERFACIAL REACTION DURING ANNEALING.

K. Heinemann, D. Bhogeswara Rao and D. L. Douglass*

Ames Research Center, NASA, Moffett Field, CA.
* University of California, Los Angeles, CA.

A certain amount of oxygen is soluble in copper (1). The attainment of the solubility limit for oxygen near the metal surface is a necessary condition for the nucleation of oxide. The rest of the unoxidized copper may remain unsaturated with oxygen even during the oxidation and is potentially capable of dissolving additional amounts of oxygen. The disappearance of copper oxide during high-temperature annealing experiments of partially oxidized copper films (2,3) as detected by TEM and TED was suggested to be due to such an oxygen dissolution process following the dissociation of copper oxide.

In order to gain more understanding of this mechanism, annealing experiments of partially oxidized (100)-oriented single crystalline copper films with various copper/oxide volume ratios were performed *in-situ* in the UHV reaction chamber of a high-resolution transmission electron microscope (2). Firstly, traces of the initial oxide, i.e., the oxide which forms during the EM specimen preparation process, would anneal out and the respective evidence in the TEM and TED would disappear within the first few minutes of annealing at 425°C and $P_{O_2} < 10^{-8}$ Pa. Secondly, a film having approximately 10 volume % of oxide initially (Fig. 1, left) required five hours of annealing under the same conditions for all evidence of the oxide to disappear (Fig. 1, right). Thirdly, in the case of a heavily oxidized film (Fig. 2), the annealing reaction is no longer marked by the complete disappearance of the oxide. Instead, voids or pin holes are formed in the oxide, mostly near the oxide-metal interface.

The disappearance of the oxide could conceivably be due to vaporization of the oxide, dissociation, or to dissociation at the oxide/metal interface enhanced by the dissolution of oxygen in the metal. Thermodynamic considerations, based on the most recent and reliable data (4), clearly indicate that neither vaporization nor dissociation are of significance at this temperature. However, the dissociation could be important at the oxide/metal interface, if the oxygen produced by the dissociation is continuously dissolving in the unoxidized copper. This process depends on the initial copper/oxide ratio and is completed either when the oxygen solubility limit in the copper is reached (Fig. 2) or when the oxygen supply is exhausted (Fig. 1), i.e., when all oxide is dissociated. The formation of voids and their spatial distribution (Fig. 2) is then due to the combined effects of dissociation of copper oxide at the oxide/metal interface and the movement of the dissociated species, i.e., of oxygen into the bulk of the unoxidized copper, and of copper into the oxide to establish in the oxide a new equilibrium concentration of cation vacancies. If the diffusion of copper is very slow, the vacancies may cluster during annealing. Upon oxidation of this sample, the pin holes disappeared, which is expected as a consequence of the rearrangement of the oxide due to the new vacancy concentration dictated by the impressed oxygen pressure. This result supports the mechanism proposed above.

1. R. W. Powers and M. V. Doyle, J. Appl. Phys., 30, 514 (1959).
2. K. Heinemann, D. B. Rao and D. L. Douglass, Oxid. of Metals, in press.
3. G. W. Simmons, D. F. Mitchell and K. R. Lawless, Surf. Sci., 8, 130 (1967).
4. S. Smoes, F. Mandy, A. Vander Auwera-Mahieu and J. Drowart, Bull. Soc. Chim. Belges, 81, 45 (1972), and JANAF Thermochemical Tables, D. R. Stull, Ed., Dow Chemical Co., Midland, Mich., 1967.

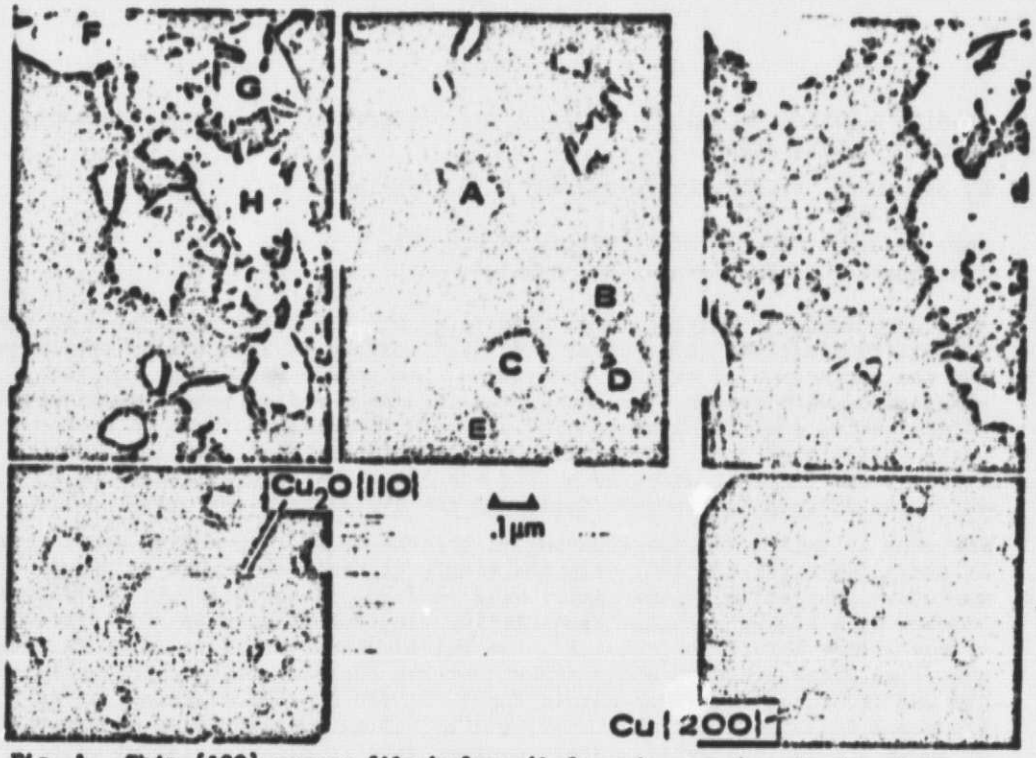

Fig. 1. Thin (100) copper film before (left and center) and after 5 hr annealing at 450°C (right). The letters A-E in the Cu (110)-selected zone dark field image (center) mark Cu_2O crystallites which disappeared during annealing. The letters F and G mark holes surrounded by Cu_2O; during annealing the Cu_2O disappeared and the holes were enlarged. H marks a hole in the oxidized film which is not surrounded by oxide and remained unchanged during annealing.

Fig. 2. Strongly oxidized (100) copper film (ratio Cu/Cu_2O = 1:3) before (a) and after 16 hr annealing at 425°C (b).

Oxidation of Metals, Vol. 10, No. 4, 1976

Oxide Removal and Desorption of Oxygen from Partly Oxidized Thin Films of Copper at Low Pressures*

D. Bhogeswara Rao,† K. Heinemann,‡ and D. L. Douglass*

Received September 30, 1975—Revised February 20, 1976

Partly oxidized copper films were annealed in a controlled vacuum of 10^{-7} Pa at a temperature of 450°C. The changes discussed below were observed in situ *with a specially designed high-resolution transmission electron microscope. The thin, (100)-oriented, single-crystal films of copper had been oxidized immediately prior to the annealing studies at the same temperature and at an oxygen partial pressure of 7×10^{-1} Pa, until the desired fraction of the copper film was converted to oxide. It was observed that the oxide disappeared during annealing as long as some copper was left unoxidized. The disappearance of the oxide is explained as being due to dissociation of the oxide at the oxide–metal toxide–metal interface followed by diffusion of oxygen into the metal and desorption of oxygen from the surface of the unoxidized copper. The rate of disappearance of the oxide was found to be proportional to the surface area of unoxidized copper, i.e., the desorption was found to be the rate-limiting step. In the case of heavily oxidized films (>50%), holes were observed to develop in the oxide near the oxide–metal interface after an annealing period of 2–3 hr. Upon resumption of the oxidation, these holes first disappeared, and the normal oxidation behavior was then resumed. The formation of holes may be explained by vacancy clustering. When completely oxidized films were annealed, recrystallization of the oxide was observed.*

KEY WORDS: desorption of oxygen; transmission electron microscopy; *in situ* oxidation studies; oxidation of thin films; nucleation of oxides.

†Materials Science Branch, NASA-Ames Research Center, Moffett Field, California.
‡Materials Department, School of Engineering and Applied Science, University of California at Los Angeles, Los Angeles, California.

*This work was performed at the Ames Research Center and funded by NASA Grants Nos. NCA2-OP390-403 and NSG-2025.

INTRODUCTION

Simmons *et al.*[1] studied both the interaction of oxygen with the surfaces of single-crystal copper using LEED and HEED and the annealing behavior of surface structures initially formed on copper. Upon annealing up to 800°C the disappearance of oxide was noted and was interpreted as being due to the presence of unsaturated copper.

Similar observations on the disappearance of appreciable amounts of oxide upon annealing partially oxidized films of copper were made by Heinemann *et al.*[2,3] It was concluded that the oxide that disappeared on annealing would provide an amount of oxygen which was several orders of magnitude more than was necessary for the staturation of the copper film. These results could not, therefore, be accounted for solely on the basis of the presence of unsaturated copper. The phenomenon appeared to be more complex and was felt to be an interesting system for further investigation for the following reasons: First, thin films of copper and cuprous oxide are used as semiconductor materials in the electronics industry. Hence, the study of material losses and compositional changes that occur upon heat treating are of importance. Second, the experimental setup is unique, as it permits the direct observation of structural changes upon annealing. Third, it was felt that through a systematic study it would become possible to explain all of the reported experimental observations. Finally, the study is one of the few ever made with thin films of single-crystal copper.

This paper summarizes experimental observations of the annealing of oxidized films of (100)-oriented single-crystal copper and offers a mechanism for the observed behavior. The annealing experiments were carried out *in situ* with samples of varying Cu_2O-Cu ratio using a high resolution transmission electron microscope (TEM).[2]

EXPERIMENTAL

The experimental apparatus employed for this work was essentially the same as that described in an earlier investigation, and the (100)-oriented single-crystal films of copper having an approximate thickness of 800 Å were prepared and oxidized using procedures that were identical to those reported earlier.[2] Oxidation was carried out at 7×10^{-1} Pa oxygen partial pressure and at 150°C until a predetermined oxide content had formed. The samples were subsequently annealed at the same temperature at 10^{-7} Pa for several hours and periodically observed *in situ*. The disappearance of Cu_2O during annealing was followed by bright field electron imaging, selected-area diffraction (SAD), and selected-zone dark field (SZDF) imaging techni-

ques. The samples were also replicated, using a platinum preshadowed carbon-replica technique, in order to study the topographical nature of the films.

RESULTS

As-Prepared Films

The surface and near-surface compositions of the as-prepared copper films were analyzed by Auger depth profiling. In addition to oxygen, considerable amounts of carbon and sulfur were noted as surface contaminants (Fig. 1). These peaks decreased rapidly during sputter etching, a normal cleaning treatment to which every specimen was subjected prior to initiation of the oxidation process. After an etching time of 10 min, corresponding to an average material removal of nearly 100 Å, the sulfur, carbon, and oxygen peaks disappeared completely and only the signals for copper were detected, indicating clean substrate conditions. Transmission electron microscope examination of some as-prepared, unetched samples in the electron microscope (EM) indicated the presence of trace amounts of oxide which might have accumulated during the EM-specimen preparation. These samples showed no oxide after annealing for 20 min at 425°C.

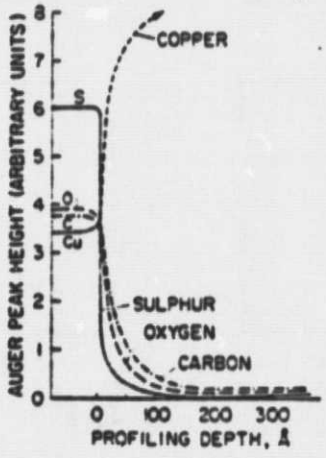

Fig. 1. Auger depth profiling analysis of as-prepared {100} copper thin films.

Annealing of Films Containing 10 vol.% of Oxide

After annealing the films to remove trace amounts of oxides, the specimen surfaces were cleaned by argon-ion sputtering and then oxidized. The oxidation was carried out for different lengths of time to form the desired vol.% of oxide. The nucleation behavior of the oxide, the number density of oxide nuclei, and the epitaxial relationships were described earlier.[2] Selected-zone dark field studies[2] established that there was no unoxidized copper left beneath the oxide nuclei, and that the oxide-particle thickness was comparable to the total thickness of the film. This permits the

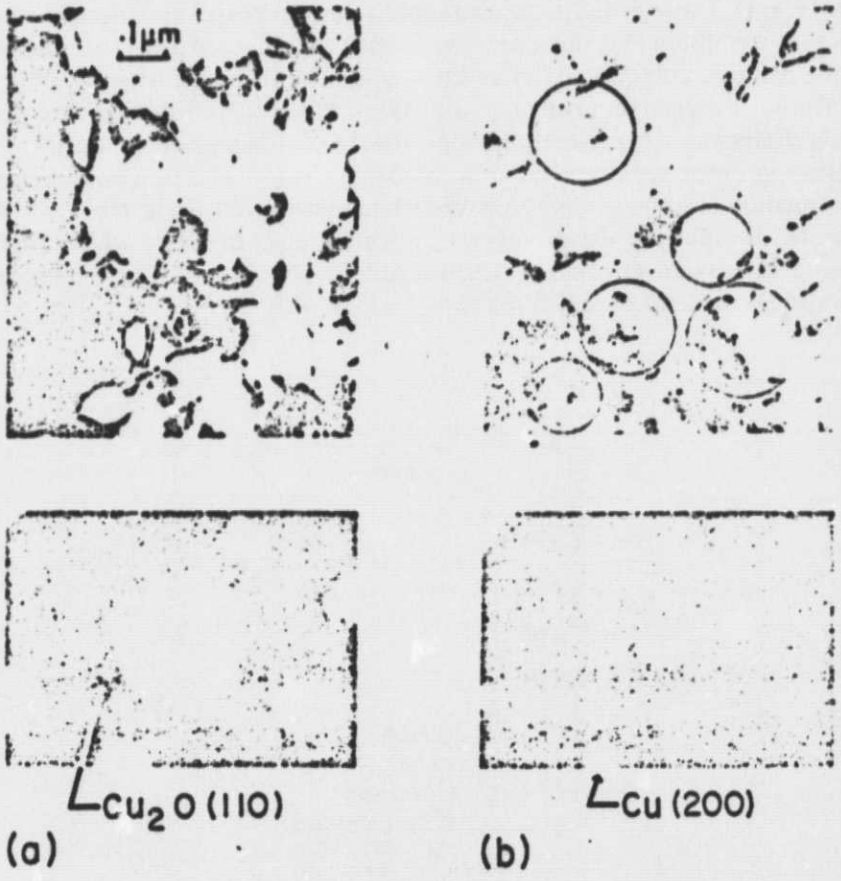

Fig. 2. Slightly oxidized {100} copper film (10 vol.%) before (a) and after (b) 5-hr annealing at 450°C. The circles mark Cu_2O crystallites which have disappeared during annealing, leaving small holes in some cases.

calculation of relative amounts of oxide present in the sample, even during the very early stages of nucleation. The surface coverage ratio of oxide to copper gives the relative amount of oxide present in the sample. A sample oxidized to approximately 10 vol.% oxide is shown in Fig. 2(a). This sample required 5 hr of annealing for all evidence of the oxide to disappear in the TEM images and SAD patterns [Fig. 2(b)]. In most cases, small holes had developed in the places where Cu_2O had been located previously [circles in Fig. 2(b)].

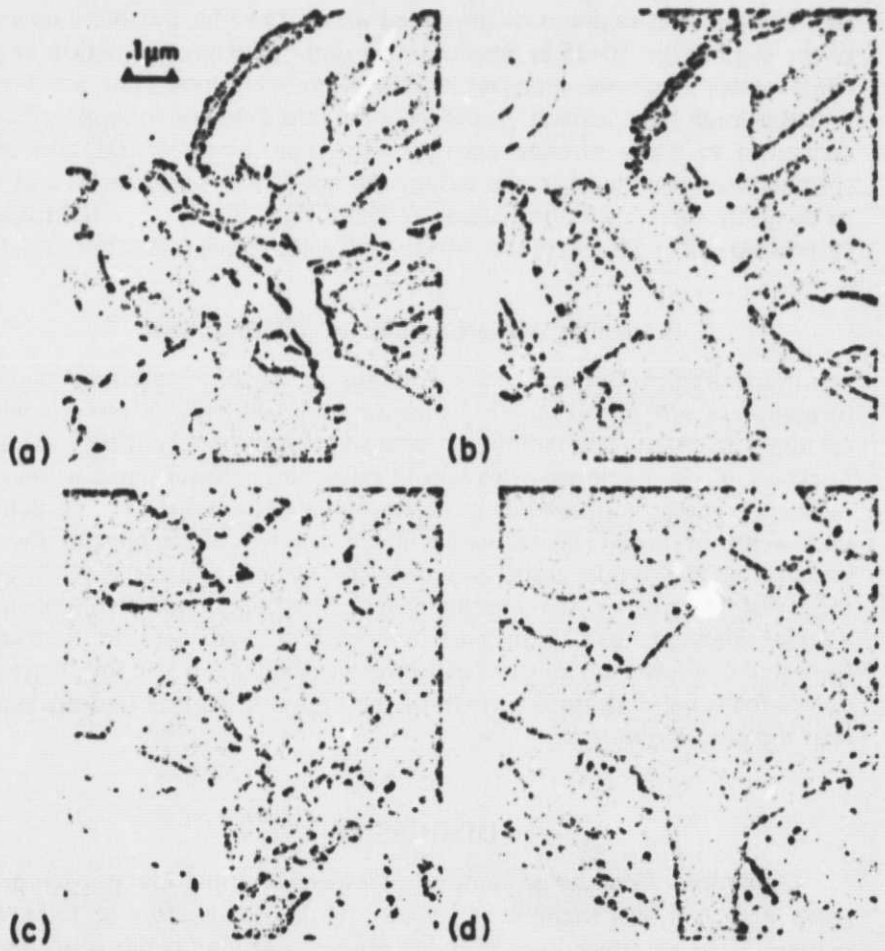

Fig. 3. Heavily oxidized (70%) {100} copper film (a), annealed 17 hr at 425°C (b, c), and reoxidized for 150 min at $6 \cdot 6 \times 10^{-1}$ Pa (5×10^{-3} Torr) oxygen partial pressure (d). (a), (b) and (c), (d) are pairs taken at the same specimen area, respectively.

Annealing of Samples Containing More Than 50% of Oxide

Heavily oxidized films, i.e., samples containing more than 50% [Fig. 3(a)] of oxide, did not exhibit a complete disappearance of oxide during annealing. Instead, voids or pinholes (seen as light areas on the micrographs) were formed in the oxide, mostly near the oxide–metal interface [Fig. 3(b), (c)]. The pinholes in the oxide appeared within 2 to 3 hr. Further annealing of the sample for 10–15 hr resulted in a slight thickness reduction of the oxide, indicating some material loss. It is probable that some additional pinholes migh have formed, but these were relatively few in number when compared to those already existing after 3 hr. Upon reoxidation of a specimen with pinholes in the oxide, the holes first disappeared and the oxide grew laterally in the usual manner [Fig. 3(d)]. This indicates a structural rearrangement of the oxide which will be discussed subsequently.

Annealing of the Completely Oxidized Films

Annealing of completely oxidized films of copper resulted again in the formation of pinholes [Fig. 4(b)]. Additionally, upon prolonged annealing for about 20 hr, the appearance of the oxide nuclei changed [Fig. 4(c)]. The thickness of the oxide particles was considerably reduced, and secondary nucleation and growth of oxide particles, assumed to be due to recrystallization, were observed. This secondary nucleation was often, but not always, initiated at the oxide grain boundaries. The nuclei grew rapidly to a thickness and size in the micron range. Micrographs of the replicated samples showed that these particles were of considerable thickness. Renewed oxidation at this stage caused no further changes in the structure, except for some additional growth of the big particles that had nucleated near the grain boundaries.

DISCUSSION

Oxidation of copper at moderate temperatures and low oxygen pressures leads to the formation of isolated oxide islands after an induction period.[2,4] The disappearance of oxide during annealing could conceivably be due to any one of the following mechanisms:

a. Dissociation of the oxide at the oxide–metal interface:

$$Cu_2O(s) \Rightarrow 2Cu(s) + O \qquad (1)$$

followed by the dissolution of oxygen into the copper matrix:

$$O + Cu(s) \Rightarrow O\,(\text{in Cu}). \qquad (2)$$

Fig. 4. Completely oxidized {100} copper film after 1-hr annealing (a), 3-hr annealing (b), and 20-hr annealing (c) at 425°C. The same specimen area is shown in all three micrographs.

b. Evaporation of the oxide:

$$Cu_2O(s) \Rightarrow Cu_2O(g) \quad (3)$$

c. Dissociation of the oxide at the vacuum–oxide interface:

$$Cu_2O(s) \Rightarrow 2Cu(s) + \tfrac{1}{2}O_2(g) \quad (4)$$

or

$$Cu_2O(s) \Rightarrow Cu(s) + CuO(g) \quad (5)$$

d. Dissociation of the oxide at the oxide–metal interface, diffusion of oxygen into the metal, followed by desorption of oxygen from the surface of the copper:

$$O\ (\text{in Cu}) \Rightarrow \tfrac{1}{2}O_2(g) \quad (6)$$

[preceded by reactions (1) and (2)].

The experimental observations were analyzed to determine which of the above processes was taking place, and are discussed consecutively in the following sections.

Dissolution of Oxygen into Unoxidized Copper

Simmons *et al.*[1] studied the annealing behavior of surface structures initially formed on copper. They found that the initial (1 × 1) oxygen structures formed on (100) copper were thermally unstable. Annealing of this structure resulted in either a clean surface at high temperatures ($T >$ 250°C) or a transformation to a (2 × 1) structure at lower temperatures. The (2 × 1) structure could be reduced to a clean surface by vacuum annealing at 400°C. However, the experimenters found it increasingly difficult to regenerate the clean surface by repeating the process. Eventually, the (2 × 1) structure was found to be stable at temperatures as high as 700°C. The results were interpreted on the basis that unsaturated copper existed and that the annealing caused a dissolution of oxygen into the copper [mechanism (1) above]. Once the region near the surface became saturated with oxygen, the oxygen diffusing to the bulk was considerably less, finally leading to the stable (2 × 1) structure. However, some experimental observations do not support the above explanation, and these are discussed below.

Simmons *et al.*[1] used bulk samples of copper, and in their case it is possible, although unlikely, that the copper was not saturated with oxygen. However, considering the extremely low solubility and a reasonable diffusion coefficient of oxygen in copper,[7,8] one would expect that in the present case with thin films of 800 Å thickness the entire copper film would be

saturated with oxygen either before the nucleation of oxide takes place or shortly thereafter. This postulate is supported by the fact that the oxidation was also marked by a long induction period of nearly 30 min; a period during which some oxygen must have gone into solution.

Furthermore, even if all of the unoxidized copper was not saturated with oxygen, the disappearance of only trace amounts of oxide could be accounted for because of the low oxygen solubility. Thus, the complete disappearance of 10 vol.% oxide during annealing could not be explained solely on the basis of oxygen dissolution in copper. If such were the case, the calculated solubility of oxygen in copper would be about 3 at.%, which is much greater than all of the reported values. The disappearance of the oxide in the present experiments can, therefore, not be attributed primarily to oxygen dissolution in the copper substrate [mechanism (a)], unless such a process is followed by some kind of oxygen diffusion mechanism toward the metal surface and subsequent desorption from the surface, as proposed in mechanism (d) above.

Evaporation of the Oxide

Since the sizes of even the smallest observed oxide nuclei were at least several hundred Å, their Cu_2O vapor pressures would not be expected to be significantly different from those of the bulk samples. It is a generally observed fact that particles with radii of more than about 50 Å behave as bulk samples and no surface tension corrections are needed. Thus, the most recent and reliable thermal data[10] on the evaporation of Cu_2O obtained for bulk samples can be applied in the present case of thin-film annealing. They clearly indicate that evaporation of Cu_2O [mechanism (b) above] is unimportant and should be considered negligible since P_{Cu_2O} is of the order of 10^{-22} atm at 750 K.

Dissociation of the Oxide at the Vacuum–Oxide Interface

The dissociation pressure of Cu_2O for reaction (4) calculated from the *JANAF Thermochemical Tables*[11] ($P_{O_2} \approx 10^{-16}$ atm) is too low to explain the observed disappearance of the oxide. Similar calculations made for reaction (5) indicate again that dissociation at the oxide–gas interface could not be expected in the reported experiments. Moreover, if dissociation of the oxide occurred, one would expect a complete disappearance of the oxide even in heavily oxidized specimens, unless the dissociation product (copper) covered the surface of the oxide, hindering further dissociation. This would then have to result in increased copper reflections in the TED mode, which was not observed. The sample containing 60% oxide exhibited a much lower rate of oxide loss than did the sample containing 10% oxide, which

therefore clearly indicates that dissociation of Cu_2O at the oxide–vacuum interface did not occur at a rate high enough to explain the experimental findings.

Desorption of Oxygen

Ranseley[8] investigated the desorption of oxygen from copper in a vacuum and found that: (a) The rate of escape of oxygen from copper was below his detection limit at temperatures below which the rate of evaporation of copper itself is significant, i.e., below 800°C; (b) the rate of evolution of oxygen remains approximately constant with time, indicating that the process of evaporation from the surface of the metal is the factor limiting the rate of oxygen desorption; (c) there is a definite accumulation of oxide at certain isolated regions on the surface; (d) the evolution of oxygen occurs preferentially from certain crystallographic planes, mainly the (100) and (110) planes; and (e) the evaporation of copper itself in vacuum, at high temperatures, is greatly enhanced by the presence of oxygen in the sample.

These observations indicate that the diffusion rate of oxygen in copper is appreciable and that no significant loss of oxygen should be expected at moderate temperatures (in the absence of reducing agents). However, the experiments[8] on which Ranseley's conclusions were based were carried out under poor vacuum conditions (10^{-3} Pa). Since low-temperature desorption phenomena are generally greatly dependent on the surface conditions and can conceivably be strongly affected by adsorption layers of residual gas molecules, there is some concern about the reliability of these early (1939) desorption studies, compromising the experimental basis for the prior hypotheses.

In fact, mechanism (d) above, which involves dissociation of Cu_2O at the Cu–Cu_2O interface, diffusion of oxygen in the metal, and desorption of oxygen from the metal surface, is the only one which may fully explain the present results. The fact that the results indicate proportionality between the rate of disappearance of Cu_2O and the amount of unoxidized copper surface area suggests that the desorption of oxygen from the surface is the limiting step which dictates the rate of dissociation at the Cu–Cu_2O interface. The number of oxygen atoms desorbing per unit time from the copper surface was found in the present study to be of the order of 10^{12} cm^{-2} sec^{-1}, an amount which is too small to be detectable by conventional weight loss measurements or by volumetric methods in a reasonable annealing time. The earlier mentioned results of Simmons *et al.*[1] can also be interpreted on the basis of this mechanism, although these authors computed an adsorption energy of oxygen on copper[9] of 110 Kcal/mole and concluded that this constitutes an insurmountable energy barrier for the desorption of oxygen at the temperatures of these experiments. However, the adsorption energy of

oxygen reported is nearly 2.5 times higher than the heat of formation of the oxide and appears to be an unreasonable value. Generally, the heat of adsorption of oxygen on metals is nearly equal to the heat of formation of their oxides or less, except in the very earliest adsorption of oxygen on the metal surface. Simmons *et al.*[1] were unable to detect the formation of oxide islands by LEED from the samples oxidized for 2 hr at a pressure of 7×10^{-1} Pa in the temperature range of 400–700°C. Examination of the samples, however, by optical and electron microscopy showed the formation of isolated nuclei of oxide. It is possible, therefore, that oxygen might have desorbed from the surface of their specimens and that the desorbed oxygen was replenished by the oxygen dissociated from the oxide.

Structural Changes

The holes which developed in heavily oxidized films (more than 50%) near the oxide–metal interface during annealing were observed to disappear upon resumption of the oxidation, which indicates some sort of structural changes.

The holes may be due to vacancy clustering. Cu_2O is a metal-deficient, *p*-type semiconductor. The concentration of the cation vacancies depends strongly on the oxygen pressure.[13] In the case of thin-film oxidation, the entire film thickness is converted to oxide, and no oxygen activity gradient exists across the film. Thus, the cation vacancy concentration is proportional to $P_{O_2}^{1/4}$, and a considerable difference in the mole fraction of cation vacancies at 7×10^{-1} Pa pressure and an annealing pressure of 10^{-8} Pa can be expected. The vacancy concentration should drop from 0.15 mole fraction to 0.003 mole fraction.[13] This reduction can occur by the precipitation of vacancies as voids. In addition, if some dissociation of the oxide takes place at the oxide–metal interface, a contraction in volume results and adds to the formation of voids. Upon resumption of the oxidation, the cation vacancy concentration in the oxide will be increased to its equilibrium value and the process will be reversed, resulting in the disappearance of the voids.

Recrystallization of the Oxide

The recrystallization of the oxide of completely oxidized films may be due to the strains present. It is known that the epitaxial growth of oxide results in strains at the oxide–metal interface. The strain is considered to be high and leads to residual stresses in the case of thin films. It is also known that the recrystallization temperature is considerably lowered in the presence of stresses. Thus, one would expect recrystallization to occur at the grain boundaries. Although the temperature does not seem to be high enough for recrystallization, no literature value is available for direct comparison.

CONCLUSIONS

The oxide nuclei that form during the oxidation of thin copper films disappear upon annealing as long as some unoxidized copper is available. The amount of oxide that disappears would provide several orders of magnitude more oxygen than would be required to saturate the unoxidized copper. Hence, the process can not be explained by the dissolution of oxygen in copper. It is proposed that oxygen desorbs from the surface of the unoxidized copper, and that the rate of desorption is rate-limiting and, therefore, proportional to the amount of unoxidized copper. Vaporization and dissociation of the oxide at the oxide–vacuum interface were eliminated as mechanisms which could describe the results.

In the case of annealing heavily oxidized films, structural changes were noticed which may be explained on the basis of vacancy clustering.

Completely oxidized films recrystallized during annealing. This is attributed to epitaxial strains present in the oxidized films.

ACKNOWLEDGMENTS

The authors are thankful to Mr. Dell P. Williams and Dr. H. R. Poppa of the Materials Science Branch, Ames Research Center, for their valuable suggestions. Thanks are due to Mr. Dale Moorhead for performing the Auger depth profiling experiments and to Mr. Dan Maghan for his technical assistance.

REFERENCES

1. G. W. Simmons, D. F. Mitchell, and K. R. Lawless, *Surf. Sci.* **8**, 130 (1967).
2. K. Heinemann, D. Bhogeswara Rao, and D. L. Douglass, *Oxid. Met.* **9**, 379 (1975).
3. K. Heinemann, D. Bhogeswara Rao, and D. L. Douglass, Proc. 33rd EMSA Meeting (1975), p. 48.
4. F. Gronlund and J. Benard, *C.R.* **240**, 624 (1955).
5. M. Hansen and K. Anderko, *Constitution of Binary Alloys* (McGraw-Hill, New York, 1958).
6. R. L. Pastorek and R. A. Rapp, *Trans. Metall. Soc. AIME* **245**, 1711 (1969).
7. A. Phillips and E. N. Skinner, *Trans. Metall. Soc. AIME* **143**, 301 (1941).
8. C. E. Ransley, *J. Inst. Met.* **65**, 147 (1939).
9. R. M. Dell, F. S. Stone, and P. F. Tiley, *Trans. Faraday Soc.* **49**, 195 (1953).
10. S. Smoes, F. Mandy, A. Vander Auwere-Mahieu, and J. Drowart, *Bull. Soc. Chim. Belg.* **81**, 45 (1972).
11. *JANAF Thermochemical Tables*, D. R. Stull, ed. (Dow Chemical Co., Midland, Mich., 1967).
12. D. F. Mitchel and K. R. Lawless, Proceedings of the Paint Research Institute, 43rd Annual Meeting of the Federation of Societies for Paint Technology, Atlantic City, N.J. (October 29, 1965).
13. P. Kofstad, in *Nonstoichiometry, Diffusion, and Electrical Conductivity in Binary Metal Oxides* (Wiley-Interscience, New York, 1972), p. 328.

(a)
1mm
(b)
(c)
(d)

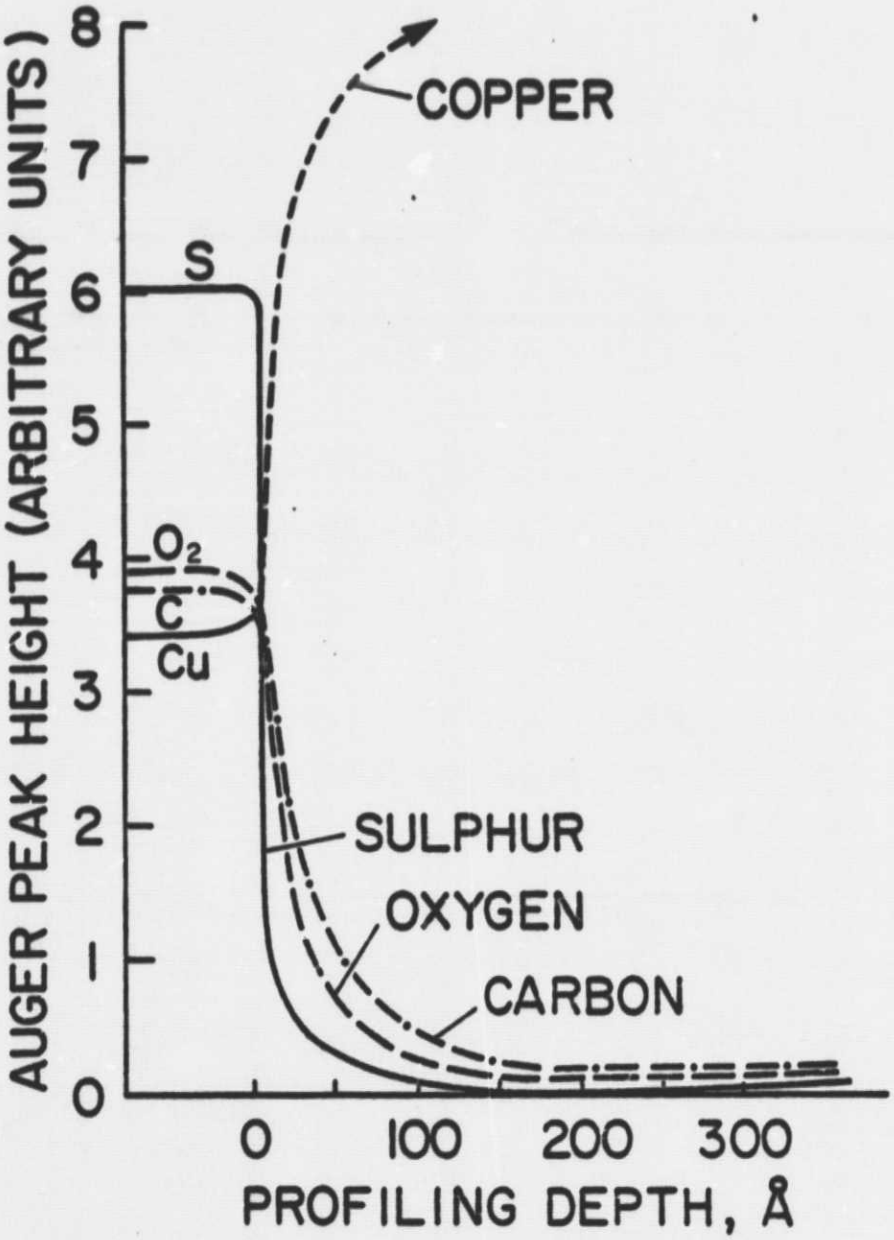
AUGER PEAK HEIGHT (ARBITRARY UNITS)
8
7
6
5
4
3
2
1
0
COPPER
S
O2
C
Cu
SULPHUR
OXYGEN
CARBON
0
100
200
300
PROFILING DEPTH, Å